

Supplementary Information

Quantification of spatial inhomogeneity in perovskite solar cells by hyperspectral luminescence imaging

Gilbert El-Hajje,^{a,b} Cristina Momblona,^c Lidón Gil-Escrig,^c Jorge Ávila,^c Thomas Guillemot,^b Jean-François Guillemoles,^d Michele Sessolo,^c Henk J. Bolink*^c and Laurent Lombez*^b

^a EDF R&D, 6 quai Watier, 78400 Chatou, France

^b Institute of Research and Development on Photovoltaic Energy (IRDEP), UMR 7174 CNRS-EDF-Chimie ParisTech, 6 quai Watier, 78400 Chatou, France. E-mail: laurent.lombez@chimie-paristech.fr

^c Instituto de Ciencia Molecular, Universidad de Valencia, C/ Catedrático J. Beltrán 2, 46980 Paterna, Spain. E-mail: henk.bolink@uv.es

^dNextPV, CNRS-RCAST joint lab, Tokyo University, Tokyo, 4-6-1 Komaba, Meguro-ku 153-8904, Japan

Absolute calibration of the photo- and electroluminescence

To calibrate the setup, we first deal with spatial uniformity and spectral correction. These relative calibrations are obtained with a halogen lamp of known spectrum, coupled into an integrating sphere with spatially homogeneous output. We therefore image the output of the sphere to calibrate the setup transmission. We then do the absolute calibration at one wavelength. To this end, we image a fiber output of NA= 0.22, in which a 783-nm laser is coupled. The NA of the fiber is smaller than the NA of the objective (0.4), ensuring us to collect all the photon flux out of the fiber. As we know the output power, we therefore have an absolute calibration of the system at the wavelength of the laser, from which we extrapolate to the entire spectral range thanks to the first relative calibration. The final result is the luminescence intensity classically expressed in absolute units of Photon flux (Photons/s) per unit of wavelength (/m) and per element of surface emission (/m^2).

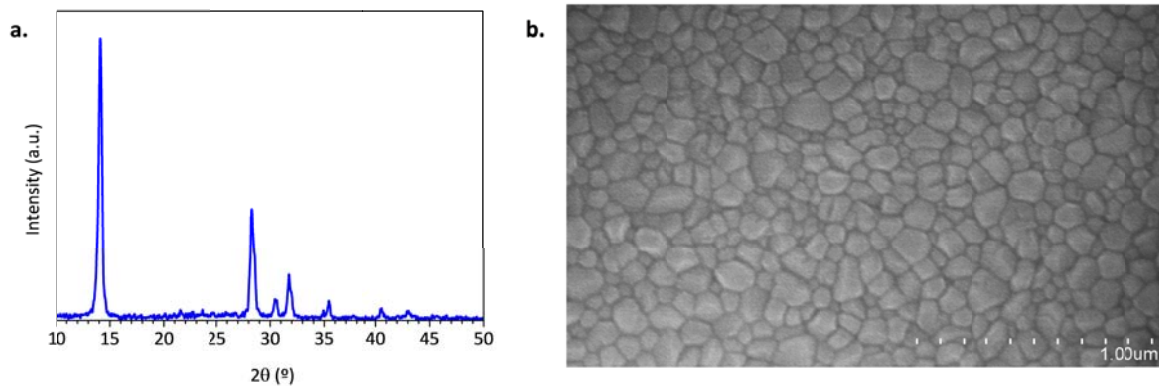


Fig. S1(a) Grazing Incidence X-ray Diffraction (GIXRD) and (b) Scanning electron microscopy (SEM) image of the surface of a vapor-deposited MAPbI₃ thin film.

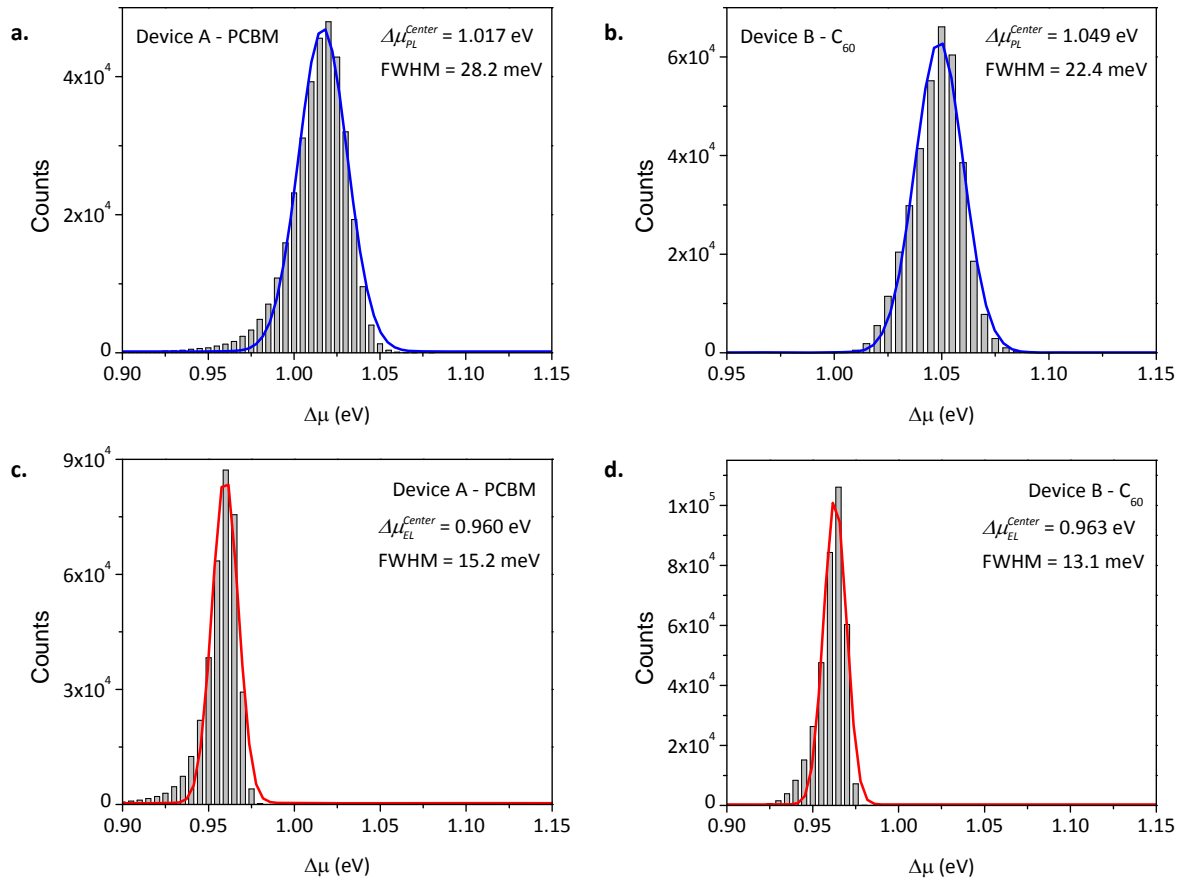


Fig. S2 Histograms fitted to a Gaussian distribution for the quasi-Fermi levels splitting ($\Delta\mu$) derived from photoluminescence (PL, blue) and electroluminescence (EL, red) hyperspectral imaging, measured for device A (a, c) and device B (b, d).

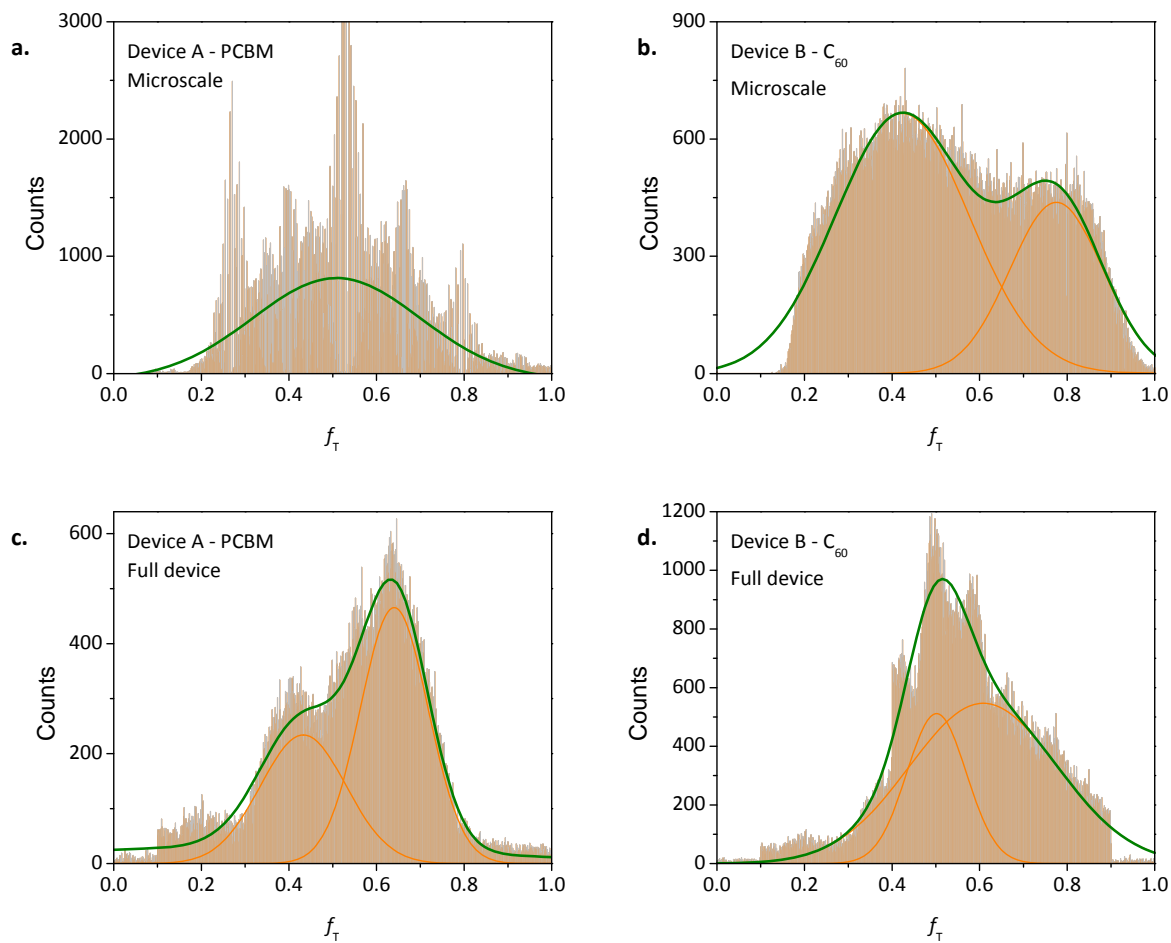


Fig. S3 Histograms fitted to a single or double Gaussian distribution of the charge carrier collection efficiency (f_T) measured for device A (a, c) and device B (b, d) at the microscale (top) and for full solar cells (bottom).

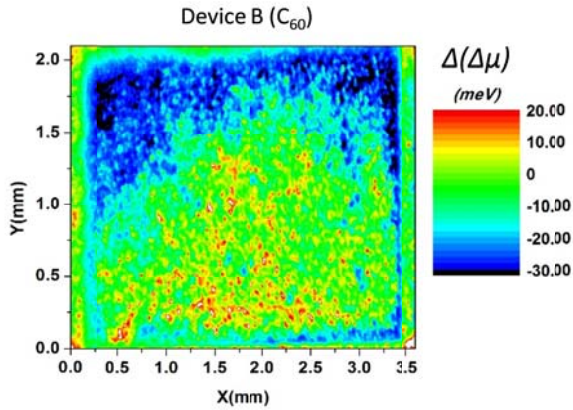


Fig. S4 Full device mapping of quasi-Fermi levels splitting fluctuations extracted from the photoluminescence hyperspectral imaging of a perovskite solar cell using C₆₀ (device B) as the electron transport layer, following the expression $\Delta(\Delta\mu) = kT \ln \left(\frac{PL(x,y)}{\text{mean}(PL(x,y))} \right)$.

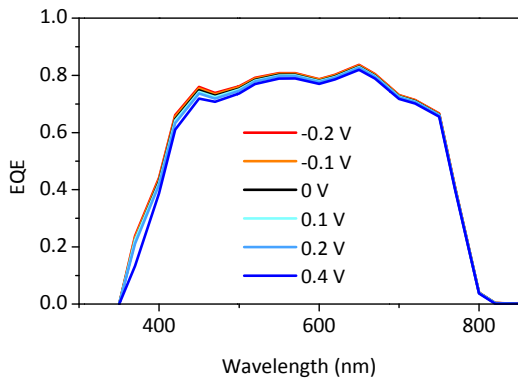


Fig. S5 The very small bias dependence of device B allows to exclude inefficient charge transport within the diode.

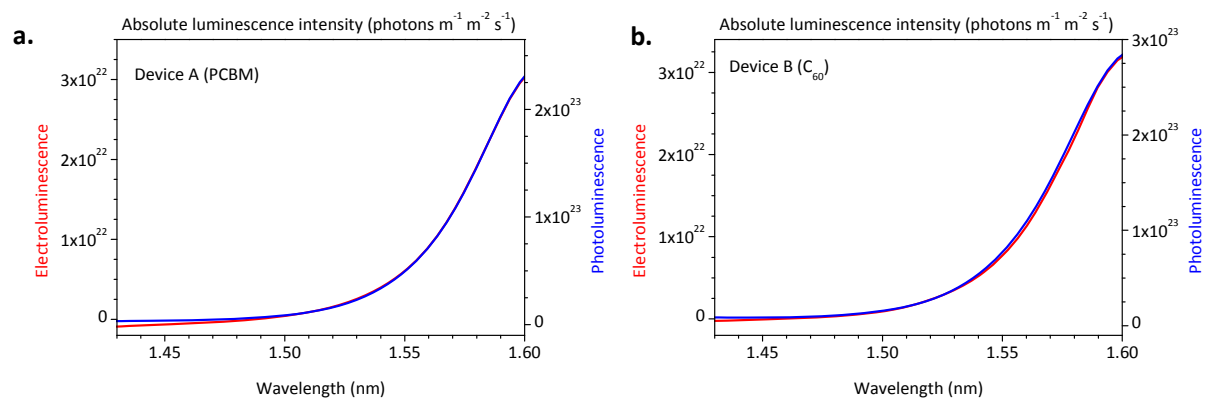


Fig. S6 A zoom is made for the low energy part of the PL (blue) and EL (red) spectra to highlight the negligible spectral variations, for both (a) device A and (b) device B.